

U N I V E R S I T Y O F R E A D I N G

ROE'S SCHEME, EULER EQUATIONS,
CARTESIAN GRIDS, NON-CARTESIAN GEOMETRIES,
RIGID WALLS - THE CONTINUING STORY.

An Appendix to Numerical Analysis Report 9/88

by

ANDREW PRIESTLEY

Numerical Analysis Report 16/88

University of Reading
Mathematics Department
P O Box 220
Whiteknights
Reading RG6 2AX

November 1988

The work reported here forms part of the research programme of the Reading/Oxford Institute for Computational Fluid Dynamics and has been supported by the S.E.R.C. Grant no. GR/E72256.

M A T H E M A T I C S D E P A R T M E N T

ROE'S SCHEME, EULER EQUATIONS,
CARTESIAN GRIDS, NON-CARTESIAN GEOMETRIES,
RIGID WALLS - THE CONTINUING STORY.

An Appendix to Numerical Analysis Report 9/88

by

ANDREW PRIESTLEY

Numerical Analysis Report 16/88

University of Reading
Mathematics Department
P O Box 220
Whiteknights
Reading RG6 2AX

November 1988

1. Introduction

The work presented here is a direct continuation of the work carried out and reported by Priestley (1988). There were certain questions raised in that report, notably about the dubious positioning of the canopy shock. Possible answers were given to the cause of the misplaced shock, none of which turned out to be right. The shock has now been repositioned into the correct place (more or less) and in this report we explain how this was done. Illustrations are also provided.

In the next section the two suggestions in the previous report are described but found to fail. Indeed a new problem is highlighted: Roe's first order scheme is usually regarded as too diffusive for many purposes but here we present a situation where it actually needs a further top up with artificial diffusion.

In Section 3 the true answer is found to be due to the fact that we were not getting as close as we thought to steady-state, and upon increasing the number of time-steps it was found that the canopy shock moved closer to where it should be. Due to this slowly moving shock our time-accurate stance must really be dropped and some special treatment is required if we are now to achieve a genuine steady-state in a reasonable amount of time. Possible options will be explored.

Finally in Section 4 we make a summary, draw conclusions and state possible avenues for further work.

2. Suggestions from Previous Work

a) In Priestley (1988) doubts were expressed over the implementation of two-dimensional rigid wall boundary conditions. It was suggested that the three-dimensional version was much simpler, and hence robust, than the more clumsy 2-D routine. The 3-D program was modified and the resulting picture, figure 1, was produced for Mach no. contours.

Although this is not successful, both programs, using different means of detecting boundary points, actually found the same numbers.

b) The other suspected source of error was that the grid was just not fine enough to place the shock accurately enough. The grid around the body was halved in both directions and early calculations produced figures 2, 3 and 4, the density, pressure coefficient and Mach number. It will be noted that the canopy shock appears to be in much the same position, although the finer grid has resulted in an increase in definition, and although the increased resolution has not solved our immediate problem the effort seems generally worthwhile. However, a close examination of the bow shock at the nose shows that there is a problem. On the coarser grid, in the previous report, some problem was detectable at the nose, but nothing on this catastrophic scale. Roberts (1988) has observed similar problems with near steady-state shocks in that he has found noise generated behind the shock. While on the coarser grid these problems were ignorable because they did not affect the solution adversely, this is now clearly not the case and something must be done.

We have overcome this problem, perhaps rather crudely, by the introduction of artificial viscosity. This aids us in two ways;

firstly in helping to damp down any noise generated at the shock, and secondly by increasing the shock width, the narrowness of the shock with Roe's scheme being a cause of the noise. This seems to work well without denegrating the solution visibly. The only question is exactly how to include the diffusion terms. From an implementational point of view we would like to include the diffusion terms explicitly as in

$$U_j^{n+1} = (1 - v\Delta_- + k\delta^2)U_j^n . \quad (2.1)$$

This can lead to unacceptably restrictive CFL limits however and is why diffusion is often treated implicitly as in

$$(1 - k\delta^2)U_j^{n+1} = (1 - v\Delta_-)U_j^n . \quad (2.2)$$

Whilst the resulting matrix equation is not the most difficult to solve for the range of k we are considering, it is an expense we could well do without.

We have therefore opted for the predictor-corrector approach demonstrated in:

$$U_j^* = (1 - v\Delta_-)U_j^n \quad (2.3a)$$

$$U_j^{n+1} = (1 + k\delta^2)U_j^* . \quad (2.3b)$$

This, to all intents and purposes, is explicit in application while having none of the same restrictive CFL limits. It also works well in practice.

3. Achieving Steady-State

Despite previous suggestions as to the reason for the misplaced canopy shock and many most helpful remarks from my colleagues, the answer turned out to be much simpler than we had supposed. Although we were well aware that the previous results were not at steady-state, as indeed the present ones aren't for that matter, we did believe that the main features of the flow had settled down. The canopy shock, and indeed all of the flow behind the bow shock, is very slow to develop. In particular, the canopy shocks moves to its final resting place extremely slowly. Just running the method for longer resulted in the canopy shock assuming something more like its correct position. We would stress again, though, that the calculation has still not reached steady-state although we are hopefully rather closer than we were.

Figures 5, 6 and 7 show density, pressure coefficient and Mach number contours for the zero incidence case and figures 8, 9 and 10 show the same for the 30° incidence case. The freestream Mach number is 8.15 in both cases.

Whilst we would argue that Roe's method on a fully cartesian grid can be a very efficient proposition, trying to achieve steady-state in a time-accurate manner is most definitely not a very efficient approach. Fortunately, although we have not implemented the ideas in this particular program, Roe's scheme can be used in a non time-accurate fashion by using local time-stepping. Dangers do exist in local time-stepping as using vastly different time-steps in neighbouring cells can lead to the production of spurious waves. However, by not allowing the time-steps to alter too drastically between neighbouring cells this can be overcome. Behind the bow shock the flow is much slower - Mach 3 is an approximate maximum and for the most part is even slower. Hence, in this region, a considerably larger time-step could be used with no ill-effect.

4. Conclusions

Using Roe's scheme on a cartesian mesh, even around non-cartesian geometries, has been shown to be a very effective means of calculating the flow around these bodies. Once time-acceleration techniques have been included it should also be a very efficient procedure for performing these types of calculations.

5. Acknowledgements

I would like to thank Dr. M.J. Baines for encouraging this work and to Mrs. Rosemary Pellew for the excellent typing.

I would also like to thank the Science and Engineering Research Council for their financial support.

6. References

PRIESTLEY, A., 1988, Roe's Scheme, Euler Equations, Cartesian Grids, Non-Cartesian Geometries, Rigid Walls And There's More. University of Reading Numerical Analysis Report 9/88.

ROBERTS, T.W., 1988, The Behaviour of Flux Difference Splitting Schemes near Slowly Moving Shock Waves. To appear in the Proceedings of the Oxford Conference on Numerical Methods in Fluid Dynamics, March 1988, (O.U.P.).

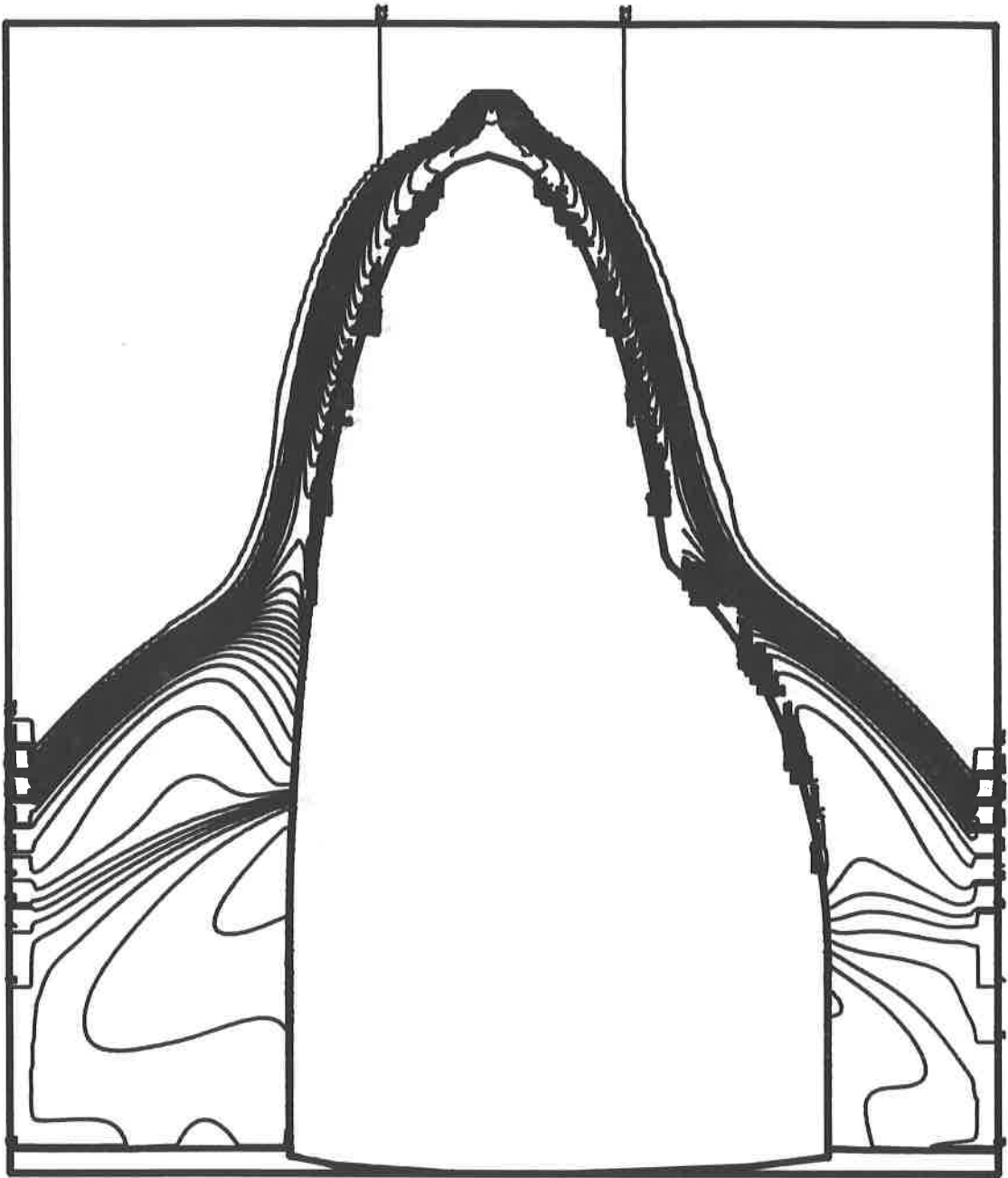


Figure 1: Mach number contours around the double ellipse?

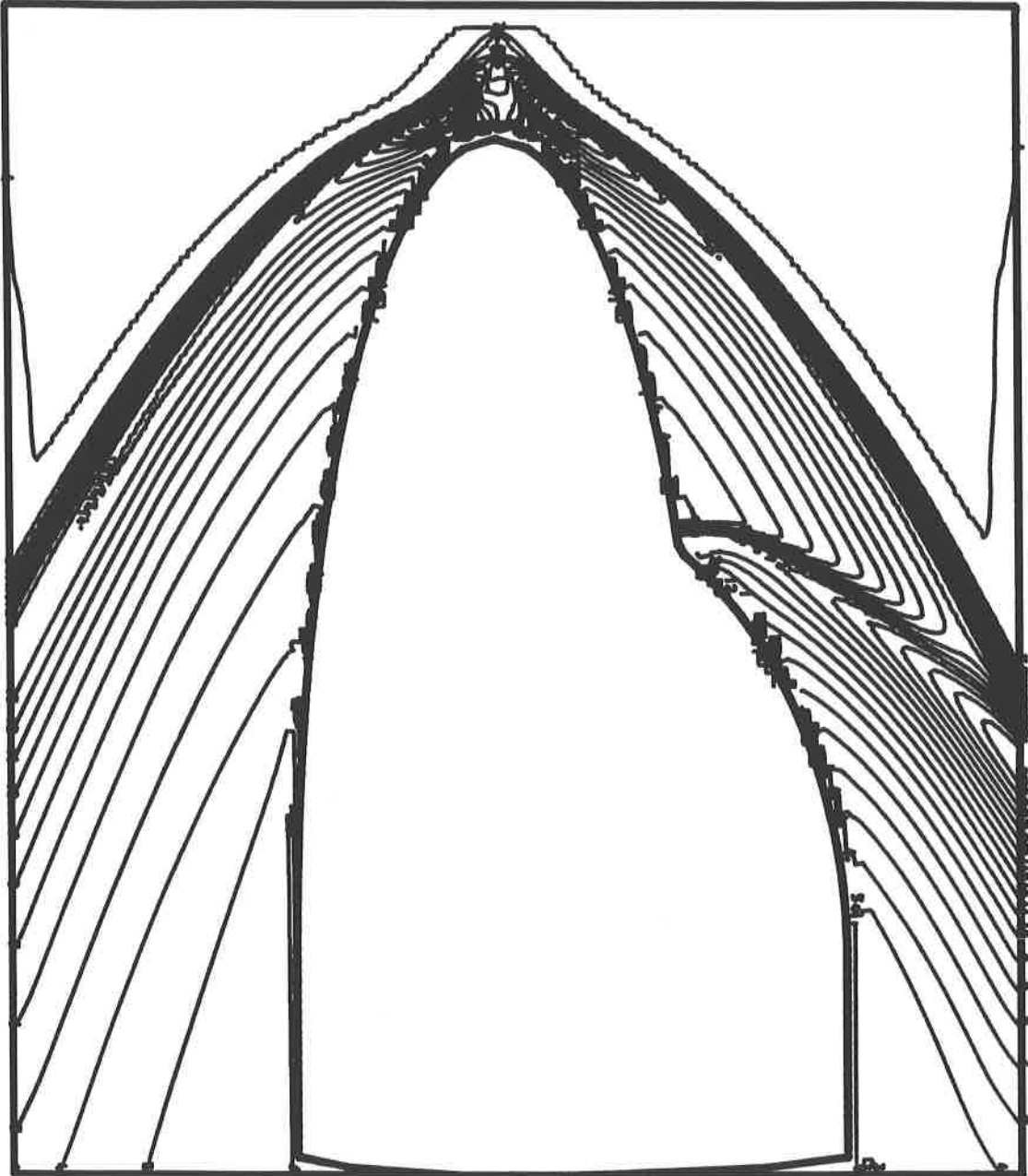


Figure 2: Density before added diffusion

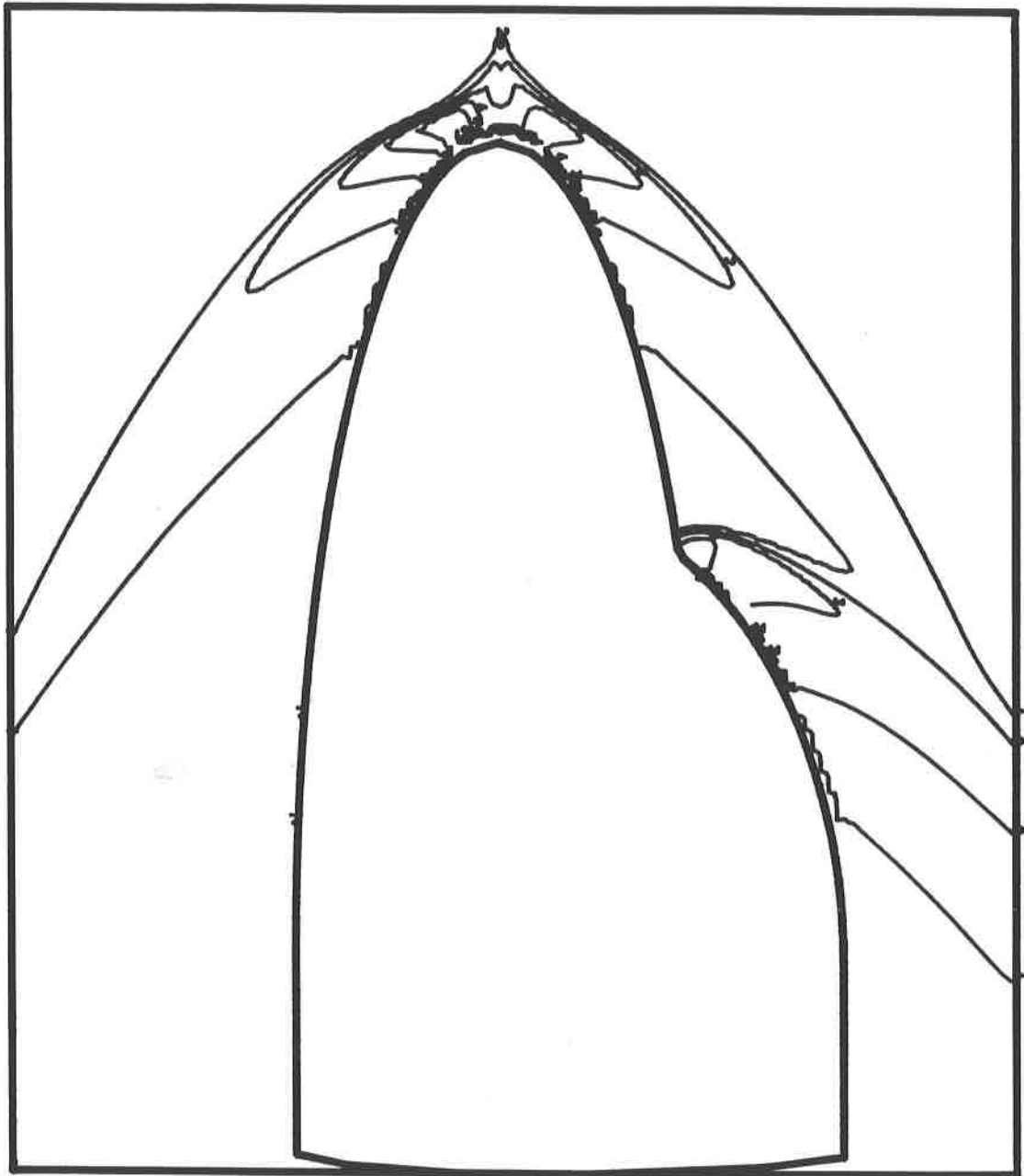


Figure 3: Pressure coefficient before added diffusion

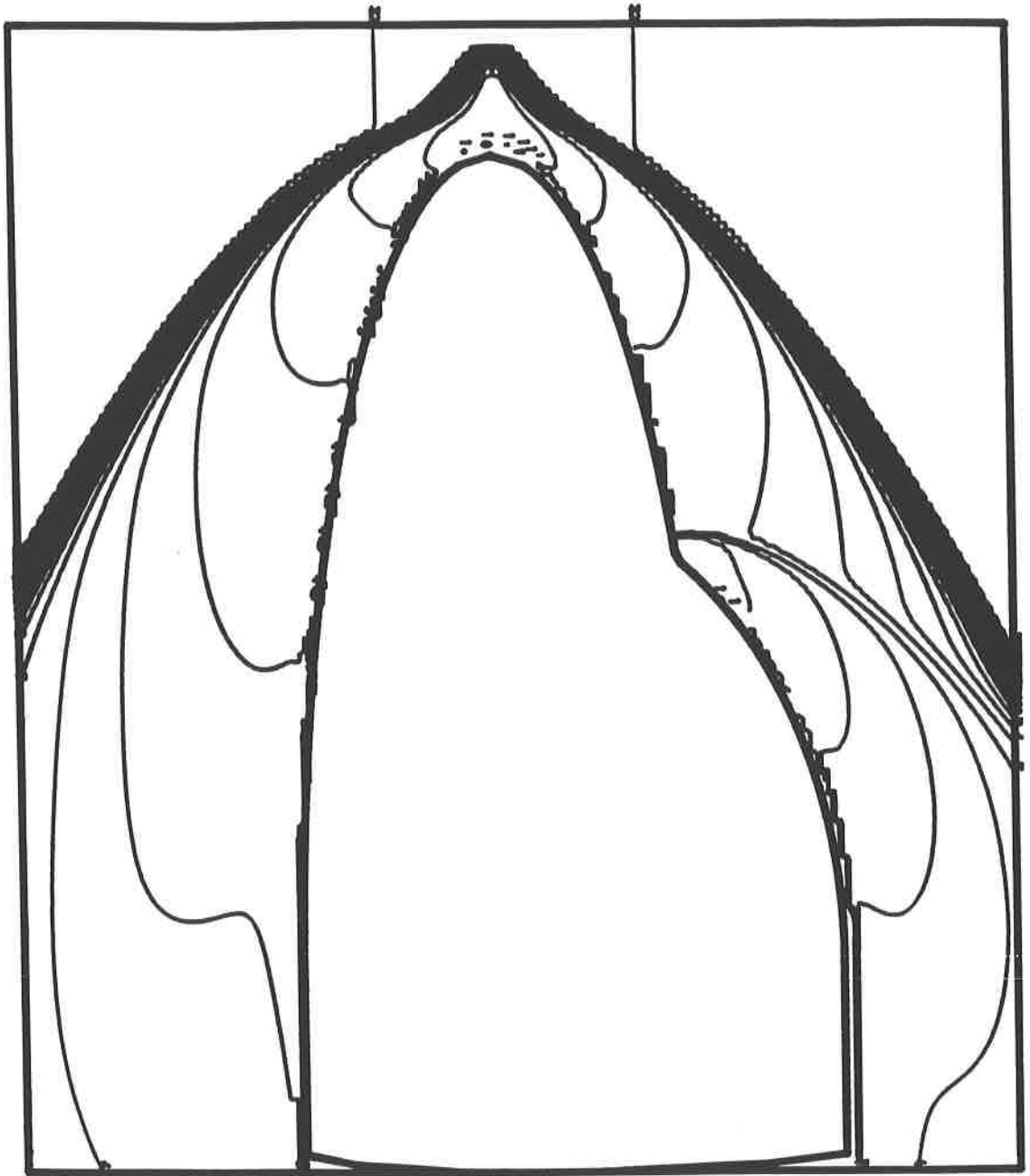


Figure 4: Mach number before added diffusion

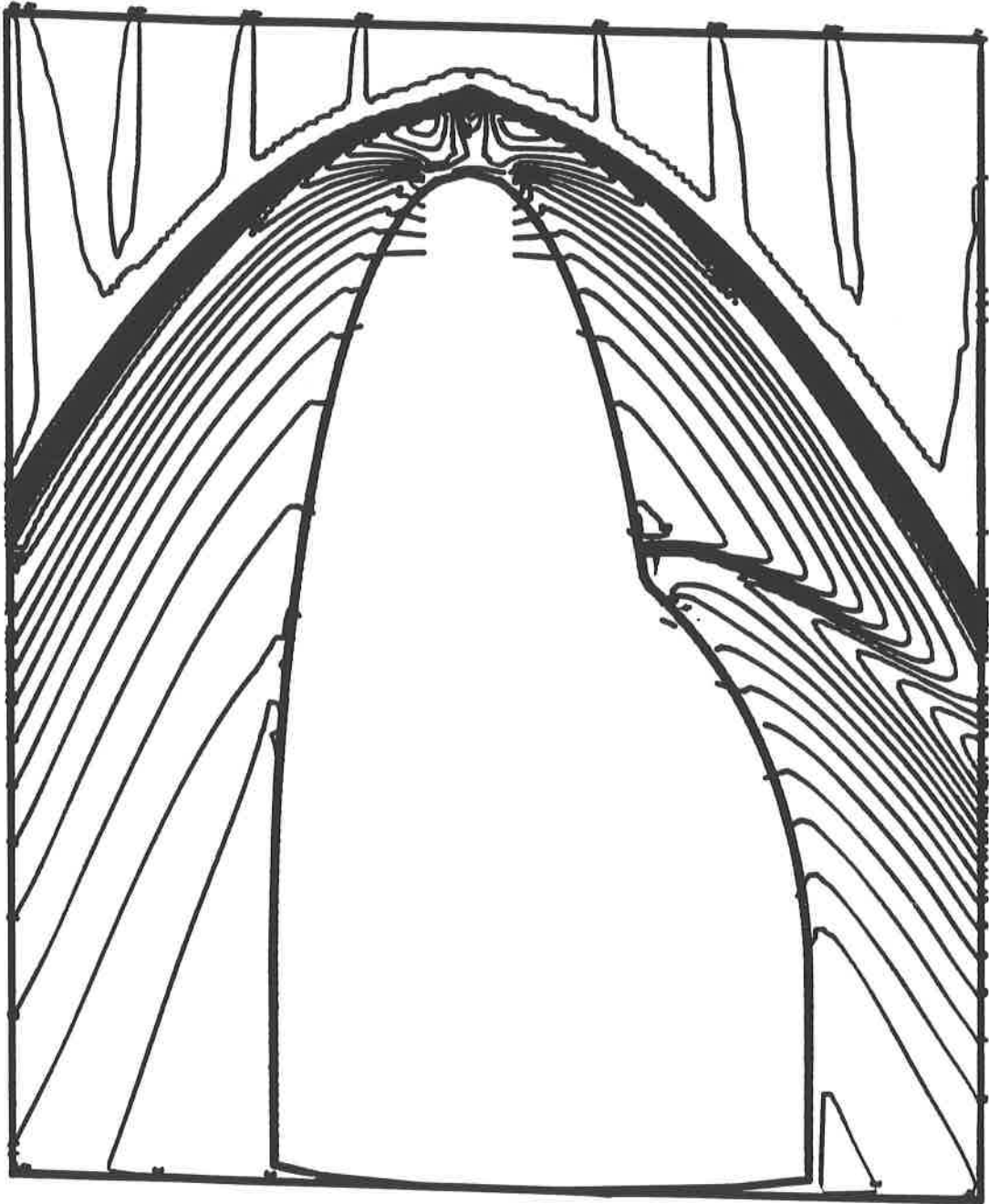


Figure 5: Density, 0° case

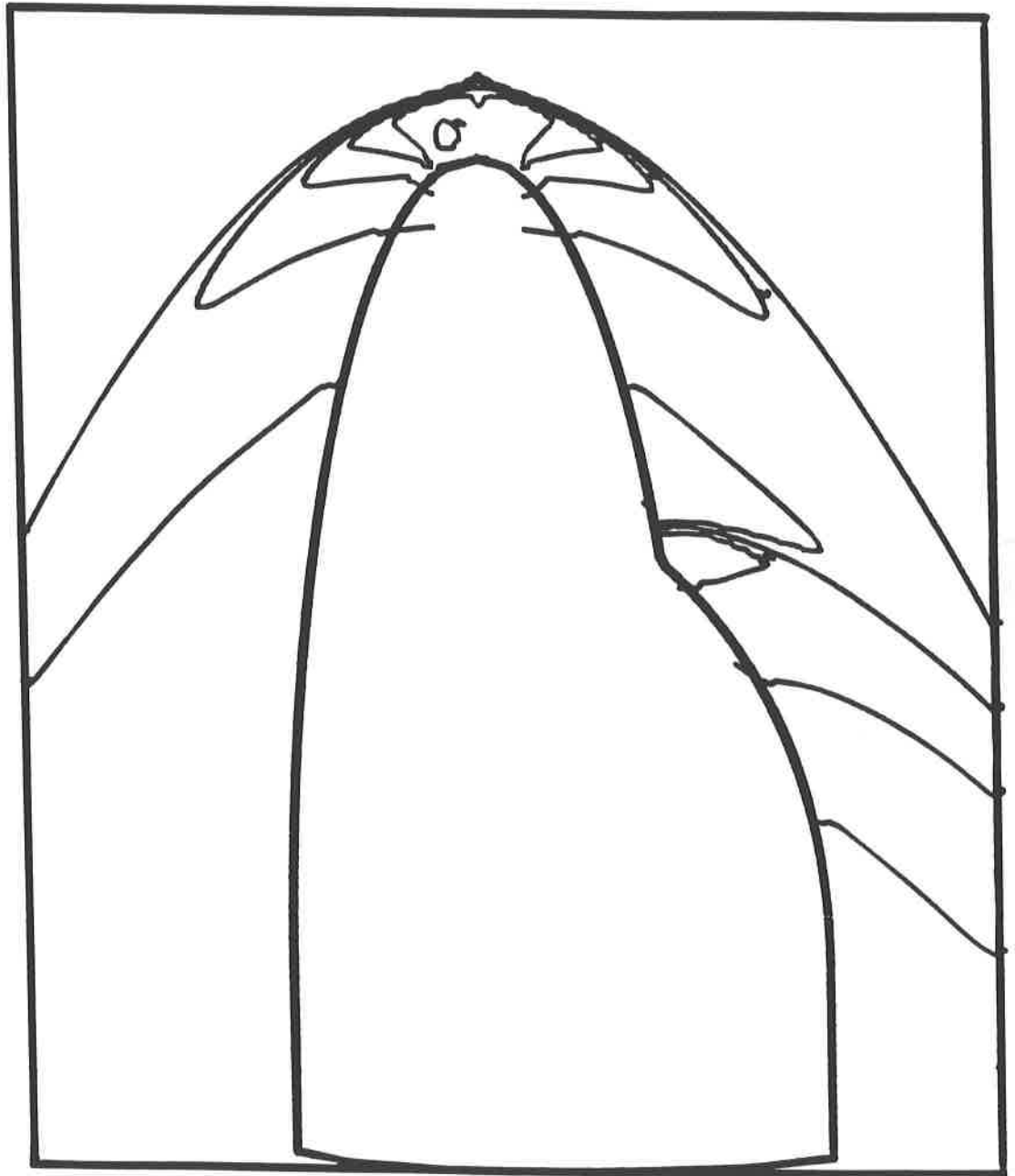


Figure 6: Pressure Coefficient 0° case



Figure 7: Mach number 0° case

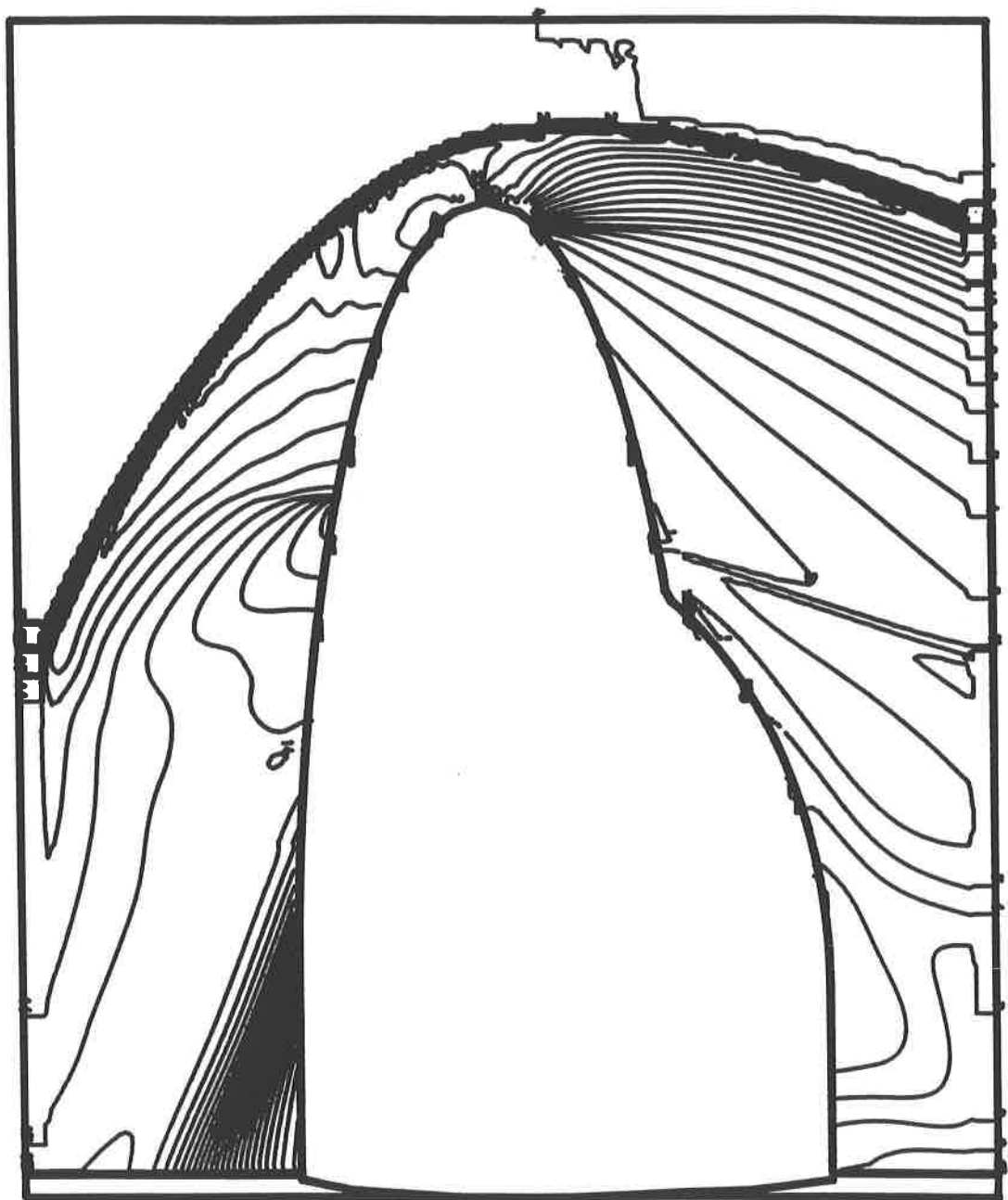


Figure 8: Density 30° case

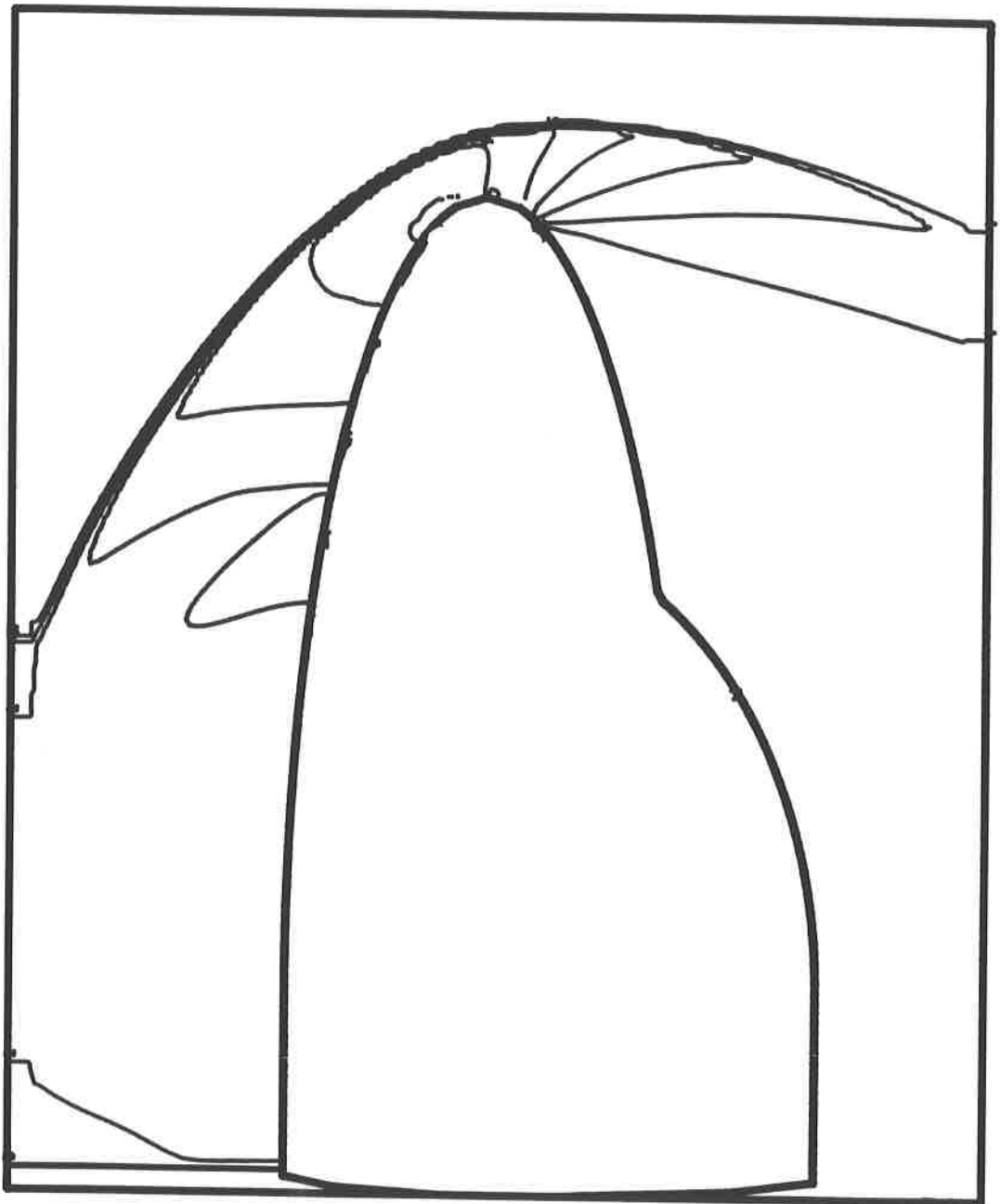


Figure 9: Pressure Coefficient 30° case



Figure 10: Mach number 30° case